

PROFESSOR GUANGMING ZHOU (Orcid ID : 0000-0001-5695-2308)

Article type : Research Article

Anti-cancer effects of CQBTO, a chloroquine and benzo(e)triazine oxide conjugate

Ziyang Guo^{a#}, Hailong Pei^{a#}, Jing Nie^a, Wentao Hu^a, Jian Zhang^a, Jiahan Ding^a, Shuxian Pan^a, Bingyan Li^a, Tom K. Hei^c, Weiqiang Chen^{b*}, Guangming Zhou^{a*}

^aState Key Laboratory of Radiation Medicine and Protection, School of Radiation Medicine and Protection, Institute of Space Life Sciences, Medical College of Soochow University, Collaborative Innovation Center of Radiological Medicine of Jiangsu Higher Education Institutions, Suzhou 215123, China;

^bInstitute of Modern Physics, Chinese Academy of Sciences, Lanzhou, China;

^cCenter for Radiological Research, College of Physician and Surgeons, Columbia University, New York, NY, USA;

These authors contributed equally.

* Corresponding Authors:

Weiqiang Chen, 509 Nanchang Rd, Lanzhou 730000, China

Phone: +86 931 4969316, E-mail: chenwq7315@impcas.ac.cn

Guangming Zhou, 199 Renai Road, Suzhou 215123, China

Phone: +86 512 6584829, E-mail: gmzhou@suda.edu.cn

This article has been accepted for publication and undergone full peer review but has not been through the copyediting, typesetting, pagination and proofreading process, which may lead to differences between this version and the Version of Record. Please cite this article as doi: 10.1111/cbdd.13477

This article is protected by copyright. All rights reserved.

ABSTRACT

Aim: Autophagy is a self-protective process, and it confers cancer cells resistance against radio-chemotherapeutics. To induce cancer cell death, a series of compounds of 3-((4-((7-chloroquinolin-4-yl)amino)butyl)amino)- 7-substituted benzo[e][1,2,4] triazine 1-oxide or CQBTO containing two critical chemical groups were designed and synthesized. One compound, BTO, yielded free radicals to trigger autophagy, and the other one, chloroquine (CQ), was an inhibitor of autophagy. We hypothesized that the compounds could kill cancer cells effectively by inducing incomplete autophagy.

Methods: *In vitro* cultured non-small cell lung carcinoma cells and primary lung tumors in mice *in vivo* were used to test the lethal effects of CQBTO on cancer cells and toxicity to normal tissues. Cell viability was examined using the CCK8 assay. Genomic instability was determined with the cytochalasin B-blocked micronucleus assay. Cell cycle distribution was analyzed by propidium iodide staining and flow cytometry. Western blotting and immunofluorescence were used to detect the induction and localization of LC3, a biomarker for autophagy.

Results: Compared with CQ, three CQBTO compounds were lethal to lung cancer cells, and CQBTO-3 was the most effective. The LD50 for CQBTO-3 was 21 μ M in A549 cells and 21.5 μ M in Calu-1 cells, which was lower than that of CQBTO-2 or CQBTO-1. Induction of LC3 foci and an increase in the LC3II/LC3I ratio demonstrated the induction of autophagy by CQBTO-3 in A549 cells, whereas no obvious micronuclei or cell cycle arrest was observed. No detectable toxicity to normal mice was observed. CQBTO-3 improved the quality of mouse life, reduced the number and size of existing tumors, and suppressed tumor formation.

Conclusion: CQBTO-3 is a potential chemical compound for lung cancer treatment.

Keywords: Autophagy; chloroquine; lung cancer; cell cycle arrest; primary mouse lung tumor.

Autophagy is an evolutionarily conserved cellular process[1]. It is an adaptive strategy by which cells recycle organelles and proteins damaged by reactive oxygen species (ROS) to survive bioenergetic stress. Persistent activation of autophagy leads to programmed cell death[2]. However, autophagy serves as a survival pathway in tumor cells treated with apoptosis activators, and the use of autophagy inhibitors such as chloroquine (CQ) in combination with therapies has been proposed for inducing apoptosis of cancer cells[3, 4].

CQ blocks the last step of the autophagy pathway by impairing autophagic protein degradation[5] [6], which leads to the accumulation of ineffective autophagosomes and the death of cells reliant on autophagy for survival[4]. High concentrations of CQ alone induce tumor cell death[7]. The combination of 3-methyladenine (3-MA) and CQ radiosensitizes the breast cancer cell line MDA-MB-231[8]. Several clinical trials of combination treatment with CQ and other chemotherapeutic drugs are underway.

ROS are constantly generated and eliminated in biological systems, and they play important roles in a variety of normal biochemical functions and abnormal pathological processes. It is possible to exploit this biochemical feature and develop novel therapeutic strategies to preferentially kill cancer cells through ROS-mediated mechanisms[9].

In the present study, we synthesized a series of compounds containing 3-[(7-chloroquine-4-amino)butyl amino]- 7- benzo[e][1,2,4]triazine- 1- O- derivatives by connecting CQ to benzo[e][1,2,4]triazine 1- oxide (BTO) with carbon chains of various length. In addition, a series of compounds were generated by modifying the BTO subunits with the same length of carbon chains. The lethal effects of these compounds against lung cancer cells and their toxicity to normal tissues were tested.

Materials and methods

Mice. Animal care and all animal experiments were performed in accordance with animal safety protocols approved by Soochow University. All *in vivo* experiments were performed using 22 ± 2 g Kunming SPF mice purchased from Shanghai SLAC Laboratory Animal Co, Ltd.

Compound synthesis and administration. CQ and BTO were purchased from Sigma-Aldrich (St. Louis, MO, USA). All the CQBTO drugs were dissolved in DMSO.

Cell culture. For *in vitro* experiments, the human non-small cell lung carcinoma cell lines A549 and Calu-1 were purchased from American Type Culture Collection in 2010 and maintained in RPMI 1640 medium (Sigma-Aldrich) supplemented with 10% fetal bovine serum (Gibco, Grand Island, NY, USA) and 10 U/mL penicillin/streptomycin [10]. Cell number was counted using a Coulter Z2 particle analyzer or Trypan Blue exclusion. Both cell lines were incubated in a humidified incubator (Thermo Scientific, NC, USA) with 5% CO₂ at 37°C.

Immunoblotting. Cultured cells were lysed in RIPA buffer (Beyotime, China). Lysates were standardized for protein content and resolved by SDS-PAGE on 12% PAGE gels. Antibodies used in this study included anti-actin (mouse monoclonal antibody, 1:10,000; Sigma-Aldrich); and anti-LC3 (rabbit polyclonal antibody, 1:2,000; CST, Danvers, MA, USA).

Immunofluorescence imaging. For GFP-LC3 fluorescence imaging, cells cultured on slides were treated with the compounds and fixed with 4% paraformaldehyde for 10 min at room temperature, permeabilized for 20 min in ethanol at -20°C, washed with PBS for 30 min, treated with 0.5% Triton for 10 min, blocked for 1 h with 5% skim milk, and stained with anti-LC3 (rabbit polyclonal antibody, 1:2,000; CST) for 2 h. The bound antibody was visualized using Alexa Fluor[®] 488 anti-mouse antibody (Abcam, NY, USA) and cell nuclei were counterstained with 4',6-diamidino-2-phenylindole (DAPI, Invitrogen, CA, USA). Slides were observed using a confocal laser scanning microscope (FV1200; Olympus, Tokyo, Japan)[11].

CCK-8 assay. Cell viability was measured using the CCK-8 assay. Briefly, 5×10^3 cells in the logarithmic growth phase in 100 μ L complete medium were seeded into a 96-well plate and incubated at 37°C in a humidified 5% CO₂ atmosphere overnight. The cells were then treated with various concentrations of the CQBTO drugs for 24 h. Then, 10 μ L of the CCK-8 reagent (Cell Counting Kit-8 DOJINDO, Rockville, MD, USA) was added to each well and incubated at 37°C for 2 h. The optical density at 450 nm (OD₄₅₀) was measured using a microplate spectrophotometer (Bio-Rad, Segrate, Italy). Cell viability was expressed as a percentage of the control.

Cell cycle analysis. At 24 h after treatment, floating and adherent cells were collected, washed with PBS, fixed with 70% ice-cold ethanol, and stained with propidium iodide (PI, 50 μ g/mL). Cell cycle progression was analyzed using a Cytomics FC500 Analyzer (Beckman Coulter, Brea, USA). Gating was used to remove cellular debris and fixation artifacts [12].

Assessment of autophagy. Antibodies that recognize the autophagy marker LC3-II (Novus Biologicals, Littleton, CO, USA) were used to detect the respective protein levels by western blotting. LC3-II was distinguished from LC3-I by size.

Statistics. Means were compared using the two-tailed Student's *t*-test. $P < 0.05$ was considered statistically significant in all calculations. All data analyses were performed using GraphPad QuickCalcs version 1 [13].

RESULTS

1. Synthesis of CQBTO

The CQBTO used in the present study was obtained as follows: 4-(aminoalkyl) amino-7-chloroquinoline derivatives were generated by the reaction of 4, 7-dichloroquinoline and alkyl diamine under conditions of high temperature. Then, the 4-(aminoalkyl) amino-7-chloroquinoline derivatives were reacted with 7-substituted- 3-chloro-1,2,4-benzotriazole-1-oxide in the presence of triethylamine to generate the desired product I (Fig. 1). While the R_2 was H and R_1 was H, then obtained the product I was CQBTO-1. While the R_2 was H and R_1 was methyl, then product I was CQBTO-2. While the R_2 was H and R_1 was Cl, the product I was CQBTO-3. For the synthesis of the 3- ((4- ((7- chloroquinolin- 4-yl)amino)butyl)amino)- 7-substituted benzo[e][1,2,4]triazine 1-oxide, chloro-1,2,4-benzotriazole- 1-oxide (50 mg, 0.275 mmol) and 4-piperazinyl- 7-chloroquinoline (68 mg, 0.275 mmol) were dissolved in 10 mL DME and 0.5 mL triethylamine. The mixture was sealed in a 50 mL bottle, heated at 80°C, and refluxed for 5 h. After the reaction was completed, the solvent was removed by rotary evaporation, and the residue was extracted with dichloromethane and water, followed by washing with a saturated salt solution and drying over anhydrous sodium sulfate. After the solvent was removed by rotary evaporation, 80 mg 4- (N-1,2,4- benzotriazole-1- oxide)-piperazinyl- 7-chloroquinoline (yield=75%) was obtained after purification by column chromatography on silica gel (PE:EA=5:1-PE:EA=2:1). ¹H NMR (400 MHz, DMSO-d₆), δ =8.74 (d, J = 5.5 Hz, 1H), 8.24-8.15 (m, 2H), 8.04 (d, J = 2.2 Hz, 1H), 7.86 (ddd, J = 8.4, 6.9, 1.4 Hz, 1H), 7.70 -7.61 (m, 2H), 7.43 (ddd, J = 8.4, 6.9, 1.2 Hz, 1H), 7.11 (t, J = 9.0 Hz, 1H), 4.08 (m, 7.6 Hz, 4H), 3.51 (t, 4H). ¹³C NMR (151 MHz, CDCl₃) δ 158.22 (s), 156.67 (s), 151.90 (s), 150.12 (s), 148.86 (s), 135.74 (s), 135.23 (s), 130.25 (s), 129.02 (s), 126.66 (d, J = 1.5 Hz), 125.39 (s), 124.89 (s), 121.89 (s), 120.50

(s), 109.30 (s), 52.04 (s), 44.04 (s), 31.94 (s), 30.21 (s), 29.71 (s), 29.38 (s). The procedures for the chemical synthesis of the other drugs can be found in Supplemental 1.

2. CQBTO-3 shows the strongest killing effect on in vitro cultured lung cancer cells.

Because inhibition of autophagy usually results in the brisk death of cancer cells, and treatment with 50 μ M CQ alone is enough to induce tumor cell death[7], we chose two concentrations (25 μ M and 40 μ M) to test the lethal effects of CQBTO compounds on two cultured human non-small cell lung carcinoma cell lines, A549 and Calu-1. As shown in Fig. 2A, CQ and CQBTO compounds at two concentrations inhibited the viability of both cell lines. The efficacy of CQBTO-1 and CQBTO-2 was similar to that of CQ, whereas CQBTO-3 showed the highest efficacy. Treatment with 25 μ M CQBTO-3 decreased A549 cell viability to $40 \pm 10\%$ and Calu-1 cell viability to $38 \pm 9\%$ of the controls, which was significantly lower than that induced by the same concentration of CQ. When cells were treated with 40 μ M CQBTO-3, more than 90% of cells lost viability, whereas 70% cells exposed to the same concentration of CQ remained active.

CQBTO-2 was selected for further comparison with CQBTO-3 regarding cancer cell lethal effects, as it showed the most similar structure to CQBTO-3 and the most similar efficacy for inhibiting cell viability to CQ and CQBTO-1. Dose response curves for cell viability were generated using the CCK-8 assay. The results showed that the lethal effects of both CQBTO-2 and CQBTO-3 were dose-dependent (Fig. 2B). The dose causing 50% lethality (LD_{50}) for CQBTO-2 was 45 μ M in A549 cells and >50 μ M in Calu-1 cells, whereas that of CQBTO-3 was 21 μ M in A549 cells and 21.5 μ M in Calu-1 cells (Table 1).

Table 1. LD_{50} of CQBTO compounds

	A549	Calu-1
CQBTO-2	45 μ M	>50 μ M
CQBTO-3	21 μ M	21.5 μ M

3. *CQBTO-3 inhibits autophagy more efficiently than CQBTO-2.*

Elevated expression of LC3, specifically the ratio of LC3II to LC3I, is a marker of autophagy[14]. We therefore detected LC3 expression in A549 (Fig. 3A) and Calu-1 cells (Fig. 3B) by western blotting. The LC3II/LC3I ratio was 0.66 ± 0.06 in control cells, 5.08 ± 3.40 in BTO treated cells, and 3.47 ± 1.85 in CQ treated cells. Treatment with CQBTO-1 or CQBTO-2 increased the ratio to 6.23 ± 3.21 or 7.50 ± 4.52 , respectively, whereas CQBTO-3 increased it to 2.52 ± 1.33 . These results indicated that CQBTO-3 inhibited autophagy.

To confirm these findings, immunofluorescence assays were performed to determine the localization of LC3. As shown in Fig. 4, LC3 foci localized to the cytoplasm of A549 cells. CQBTO-3 induced the formation of LC3 loci at a considerably lower rate than CQ or CQBTO-2 treatment, which was consistent with the relatively low LC3II/LC3I ratio in cells exposed to CQBTO-3. Starvation and exposure to ionizing radiation induce autophagy. Treatment with CQBTO-3 reduced the formation of LC3 foci induced by starvation or radiation exposure. Next, cell cycle distribution was analyzed by flow cytometry. As shown in Fig. 5, CQ, CQBTO-2, or CQBTO-3 induced G1 block in both cell lines, and CQBTO-2 had a stronger effect on inducing G1 phase block than CQBTO-3. Taken together, these findings indicated that CQBTO-3 inhibited autophagy more efficiently than CQBTO-2.

4. *CQBTO-3 shows the strongest effects in a mouse lung cancer model.*

A urethane-induced primary mouse lung tumor model was used to explore the efficacy of CQBTO-3 for the treatment of lung cancer. Mice bearing lung primary tumors were divided into five groups: Ctrl, BTO, CQ, CQBTO-3, and CQBTO-2 groups. Mice were treated with five drugs at a dose of 1 mM (200 μ L) once a day for 30 days. As shown in Fig. 6A, one of eight mice treated with CQBTO-3 died after 30 days, whereas four of eight mice in the Ctrl group, two in the CQ group, and one in the CQBTO-2 group died after 30 days. None of the mice in the CQBTO-3 group died after 28 days of treatment. These data suggested that CQBTO-3 was effective in killing primary mouse lung tumors.

There was no significant weight loss in all the mouse groups (Fig. 6B). In the CQBTO-3 group, the size and number of tumors were smaller than those of the other groups (Fig. 6C). As shown in Fig. 6D, there were no visible changes in organs such as the liver, spleen, and kidney. Peripheral blood cells were detected by automated hematology (Fig. 6E), BTO, CQ, or CQBTO decreased the levels of HGB, MCHC, and MCH, whereas there were no

significant differences between the effects of CQBTO-3 and CQBTO-2. Compared with the other groups, mice in the CQBTO-3 group were more active, suggesting that CQBTO-3 can improve the quality of life of mice bearing lung tumors.

Discussion

Chemotherapeutic drugs are often toxic. Therefore, it is important to develop antitumor drugs possessing strong lethal effects with little toxicity. In the present study, we chemically combined CQ with BTO, a ROS generator, with carbon chains and tested its lethal effects on cancer cells and in a mouse lung cancer model. Among the synthesized CQBTO compounds, CQBTO-3 showed promise for the treatment of lung tumors, with a strong lethal effect and little toxicity.

The antitumor mechanism of CQ involves the induction of apoptosis[15] and autophagy[16, 17], scavenging of tumor stem cells[18, 19], and vascular normalization[20]. CQ is therefore a promising agent for the treatment of cancer.

Autophagy is a stabilizing process that acts via organelle degradation. Autophagy has a dual purpose in processing useless or damaged organelles and helping cells survive unfavorable conditions. This mechanism has two different effects on cancer cells: it can cause cancer cell death, and it can help tumor cells resist severe environmental conditions and promote tumor cell growth.

The use of CQ alone can inhibit the proliferation of tumor cells both *in vitro* and *in vivo*. [21]. Although CQ can cause tumor cell death directly, large doses of CQ can cause liver damage. [22] Therefore, although large doses of CQ can inhibit autophagy and induce the direct death of tumor cells, its clinical application in the treatment of cancer is limited. [23]

The structure of CQBTO has a critical impact on its lethal effects on cancer cells. The length of the carbon chain between CQ and BTO is a critical factor, as the lethal effects increase with chain length. The strong lethal effects of CQBTO-3 were correlated with its long carbon chain, which is associated with a low ROS quenching ability among the CQ group. In addition, the substituent group plays an important role. CQBTO compounds are characterized by differences in the substituent group, 7-benzo[e][1,2,4]triazine 1-oxide: the group is hydro- for CQBTO-1, methyl- for CQBTO-2, and chloro- for CQBTO-3. The strong lethal effects of CQBTO-3 may be attributed to the impact of the chloro- group on promoting the production of ROS [16, 23].

In summary, CQBTO-3 is a promising agent for the treatment of lung tumors, showing a strong lethal effect and little toxicity. Additional experiments are needed before this agent can be used in clinical practice.

Disclosure of potential conflicts of interest

The authors declare no competing financial interests.

Author contributions

Ziyang Guo and Hailong Pei conducted most of the experimental studies, data analysis, and drafted the manuscript. These authors contributed equally to this work. Drs. Wentao Hu and Jian Zhang provided technical help and performed experiments. Jiahan Ding helped with animal experiments. Jing Nie managed laboratory work, including quality assurance and control. Drs. Bingyan Li and Tom K. Hei provided valuable suggestions and revised the English writing. Dr. Weiqiang designed and synthesized the chemicals. Dr. Guangming Zhou designed the study and organized the research.

Funding

This work was supported by the National Natural Science Foundations of China (81602794, 81773463, and 81673151), China Postdoctoral Science Foundation (2017T100399), and Natural Science Foundations of Jiangsu Province (BK20160334). This work was also supported by “A Project Funded by the Priority Academic Program Development of Jiangsu Higher Education Institutions (PAPD)”.

Figure legends

Figure 1. Synthesis of CQBTO compounds. (A) The synthesis of 3-[(7-chloroquinolin-4-amino) alkylamino]-7-substituted-benzo [e] [1,2,4] triazine-1-oxo. (B) Chemical structural formula of CQBTO-1, CQBTO-2, and CQBTO-3.

Figure 2. The lethal effects of CQBTO compounds on two kinds of *in vitro* cultured human non-small cell lung carcinoma cell lines. (A) CQ and CQBTO compounds at two concentrations inhibited the viability of both cell lines (A549 and Calu-1) as measured by the CCK-8 assay. (B) Dose response curves for cell viability were generated based on the results of the CCK-8 assay in both cell lines. The error bars denote the mean \pm SE derived from three independent experiments.

Figure 3. The expression of LC3 in A549 (A) and Calu-1 cells (B) measured by western blotting in cells treated with different drugs (n = 3). The error bars denote the mean \pm SE from three independent experiments.

Figure 4. Localization of LC3 in A549 cells. Immunofluorescence analysis was used to determine the localization of LC3 in A549 cells after different treatments.

Figure 5. (A) Flow cytometry showing significant increases in the percentage of cells in the G1 phases when the cells were treated with CQ, CQBTO-2, or CQBTO-3 in both cell lines. (B) Cell cycle distribution measured with flow cytometry. The error bars denote the mean \pm SE derived from three independent experiments.

Figure 6. Efficacy of CQBTO-3 in a urethane-induced mouse lung cancer model. The mice bearing lung primary tumors were divided into five groups: Ctrl group, BTO group, CQ group, CQBTO-3 group, and CQBTO-2 group. Mice were treated with five different drugs at 1 mM (200 μ L) once a day for 30 days. (A) One of eight mice died in 30 days in the CQBTO-3 group, whereas four of eight mice in the Ctrl group, two in the CQ group, and one in the CQBTO-4 group died in 30 days. None of the mice in the CQBTO-3 group died after 28 days. (B) No significant weight changes were observed in all the mouse groups. (C) Tumor size of the different groups. (D) Changes in organ index including liver, spleen, and kidney. (E) The peripheral blood cells were detected by automated hematology. The levels of HGB, MCHC, and MCH decreased after treatment with BTO, CQ, or CQBTO.

Reference

- [1] E. Wirawan, T. Vanden Berghe, S. Lippens, P. Agostinis, P. Vandenabeele, Autophagy: for better or for worse, *Cell research*, 22 (2012) 43-61.
- [2] L. Yu, A. Alva, H. Su, P. Dutt, E. Freundt, S. Welsh, E.H. Baehrecke, M.J. Lenardo, Regulation of an ATG7-beclin 1 program of autophagic cell death by caspase-8, *Science*, 304 (2004) 1500-1502.
- [3] R.K. Amaravadi, D. Yu, J.J. Lum, T. Bui, M.A. Christophorou, G.I. Evan, A. Thomas-Tikhonenko, C.B. Thompson, Autophagy inhibition enhances therapy-induced apoptosis in a Myc-induced model of lymphoma, *The Journal of clinical investigation*, 117 (2007) 326-336.
- [4] J.J. Lum, D.E. Bauer, M. Kong, M.H. Harris, C. Li, T. Lindsten, C.B. Thompson, Growth factor regulation of autophagy and cell survival in the absence of apoptosis, *Cell*, 120 (2005) 237-248.
- [5] V.R. Solomon, H. Lee, Chloroquine and its analogs: a new promise of an old drug for effective and safe cancer therapies, *European journal of pharmacology*, 625 (2009) 220-233.
- [6] H. Glaumann, J. Ahlberg, Comparison of different autophagic vacuoles with regard to ultrastructure, enzymatic composition, and degradation capacity--formation of crinosomes, *Experimental and molecular pathology*, 47 (1987) 346-362.
- [7] K.H. Maclean, F.C. Dorsey, J.L. Cleveland, M.B. Kastan, Targeting lysosomal degradation induces p53-dependent cell death and prevents cancer in mouse models of lymphomagenesis, *The Journal of clinical investigation*, 118 (2008) 79-88.
- [8] H. Chaachouay, P. Ohneseit, M. Toulany, R. Kehlbach, G. Multhoff, H.P. Rodemann, Autophagy contributes to resistance of tumor cells to ionizing radiation, *Radiotherapy and oncology : journal of the European Society for Therapeutic Radiology and Oncology*, 99 (2011) 287-292.
- [9] H. Pelicano, D. Carney, P. Huang, ROS stress in cancer cells and therapeutic implications, *Drug resistance updates : reviews and commentaries in antimicrobial and anticancer chemotherapy*, 7 (2004) 97.
- [10] N. Ding, H. Pei, W. Hu, J. He, H. Li, J. Wang, T. Wang, G. Zhou, Cancer risk of high-charge and -energy ions and the biological effects of the induced secondary particles in space, *Rendiconti Lincei*, 25 (2014) 59-63.
- [11] W. Hu, H. Pei, H. Li, N. Ding, J. He, J. Wang, Y. Furusawa, R. Hirayama, Y. Matsumoto, C. Liu, Effects of shielding on the induction of 53BP1 foci and micronuclei after Fe ion exposures, *J Radiat Res.*, 55 (2013) 10-16.
- [12] H. Pei, J. Zhang, J. Nie, N. Ding, W. Hu, J. Hua, R. Hirayama, Y. Furusawa, C. Liu, B. Li, RAC2-P38 MAPK-dependent NADPH oxidase activity is associated with the resistance of quiescent cells to ionizing radiation, *Cell cycle*, 16 (2017) 113-122.

- [13] H. Pei, W. Chen, W. Hu, M. Zhu, T. Liu, J. Wang, G. Zhou, GANRA-5 protects both cultured cells and mice from various radiation types by functioning as a free radical scavenger, *Free Radical Research*, 48 (2014) 670.
- [14] D.J. Klionsky, F.C. Abdalla, H. Abeliovich, R.T. Abraham, A. Acevedo-arozena, K. Adeli, L. Agholme, M. Agnello, P. Agostinis, J.A. Aguirreghiso, Guidelines for the use and interpretation of assays for monitoring autophagy, (2015).
- [15] P.D. Jiang, Y.L. Zhao, X.Q. Deng, Y.Q. Mao, W. Shi, Q.Q. Tang, Z.G. Li, Y.Z. Zheng, S.Y. Yang, Y.Q. Wei, Antitumor and antimetastatic activities of chloroquine diphosphate in a murine model of breast cancer, *Biomedicine & pharmacotherapy = Biomedecine & pharmacotherapie*, 64 (2010) 609.
- [16] A. Yang, A.C. Kimmelman, Inhibition of autophagy attenuates pancreatic cancer growth independent of TP53/TRP53 status, *Autophagy*, 10 (2014) 1683-1684.
- [17] S. Avniel-polak, G. Leibowitz, Y. Riahi, B. Glaser, D.J. Gross, S. Grozinsky-glasberg, Abrogation of Autophagy by Chloroquine Alone or in Combination with mTOR Inhibitors Induces Apoptosis in Neuroendocrine Tumor Cells, *Neuroendocrinology*, 103 (2015).
- [18] X. Li, M.T. Lewis, J. Huang, C. Gutierrez, C.K. Osborne, M.F. Wu, S.G. Hilsenbeck, A. Pavlick, X. Zhang, G.C. Chamness, Intrinsic resistance of tumorigenic breast cancer cells to chemotherapy, *Journal of the National Cancer Institute*, 100 (2008) 672.
- [19] C.J. Creighton, X. Li, M. Landis, J.M. Dixon, V.M. Neumeister, A. Sjolund, D.L. Rimm, H. Wong, A. Rodriguez, J.I. Herschkowitz, Residual breast cancers after conventional therapy display mesenchymal as well as tumor-initiating features, *Proceedings of the National Academy of Sciences of the United States of America*, 106 (2009) 13820.
- [20] H. Maes, A. Kuchnio, A. Peric, S. Moens, K. Nys, K. Debock, A. Quaegebeur, S. Schoors, M. Georgiadou, J. Wouters, Tumor Vessel Normalization by Chloroquine Independent of Autophagy, *Cancer cell*, 26 (2014) 190.
- [21] H.U. Tao, L.I. Pei, Z. Luo, X. Chen, J. Zhang, C. Wang, P. Chen, Z. Dong, Chloroquine inhibits hepatocellular carcinoma cell growth in vitro and in vivo, *Oncology reports*, 35 (2016) 43-49.
- [22] H.M. Ni, H. Jaeschke, W.X. Ding, Targeting autophagy for drug-induced hepatotoxicity, *Autophagy*, 8 (2012) 709-710.
- [23] T. Kimura, Y. Takabatake, A. Takahashi, Y. Isaka, Chloroquine in cancer therapy: a double-edged sword of autophagy, *Cancer research*, 73 (2013) 3-7.

Figure 1

(A)

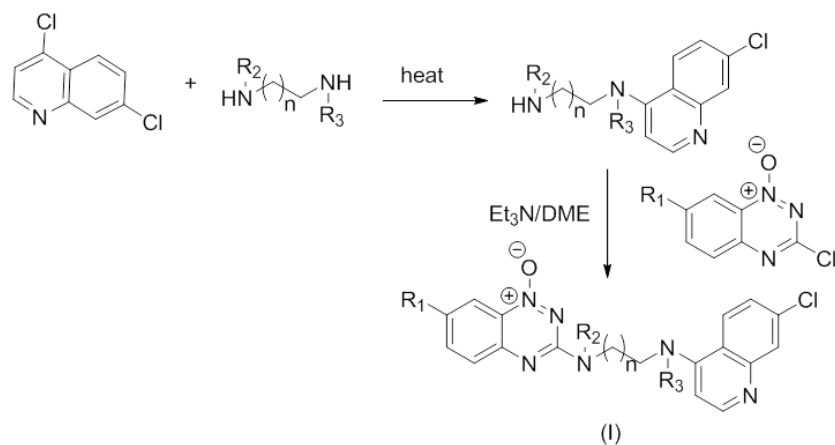


Figure 1

(B)

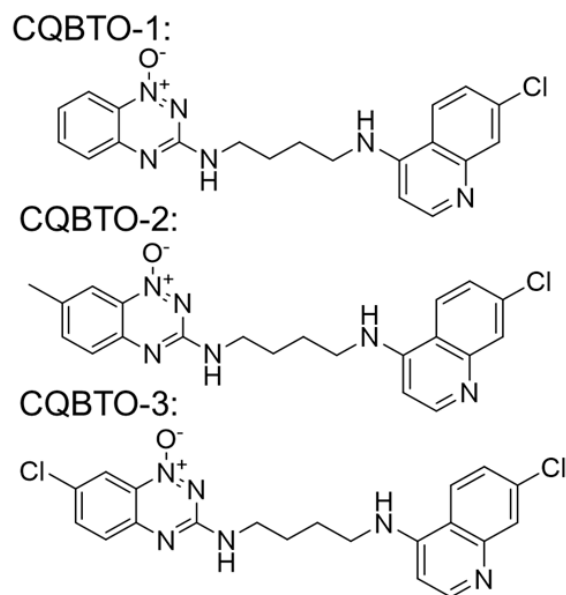


Figure 2

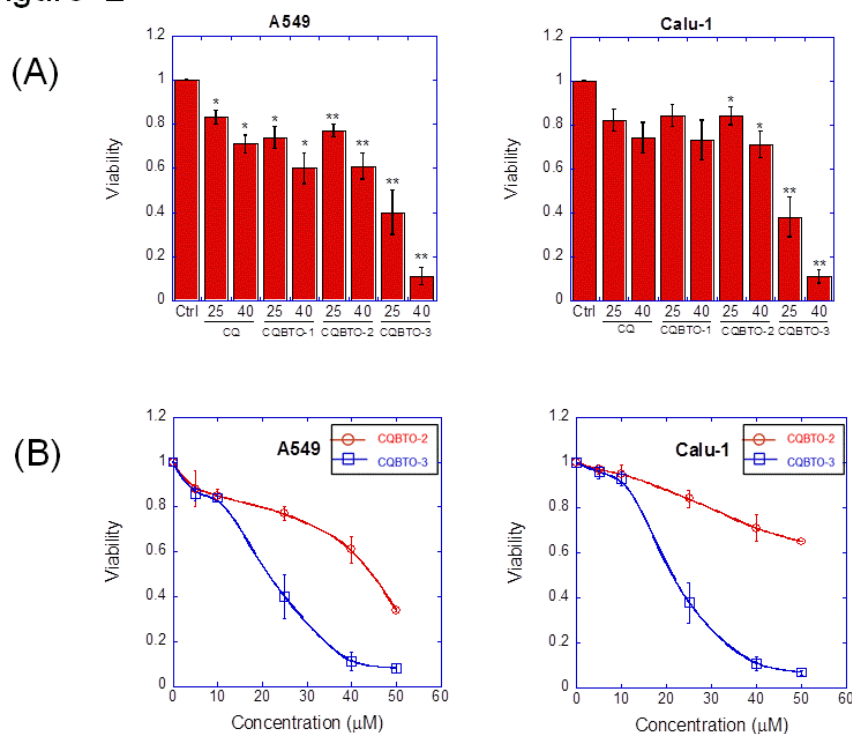


Figure 3:

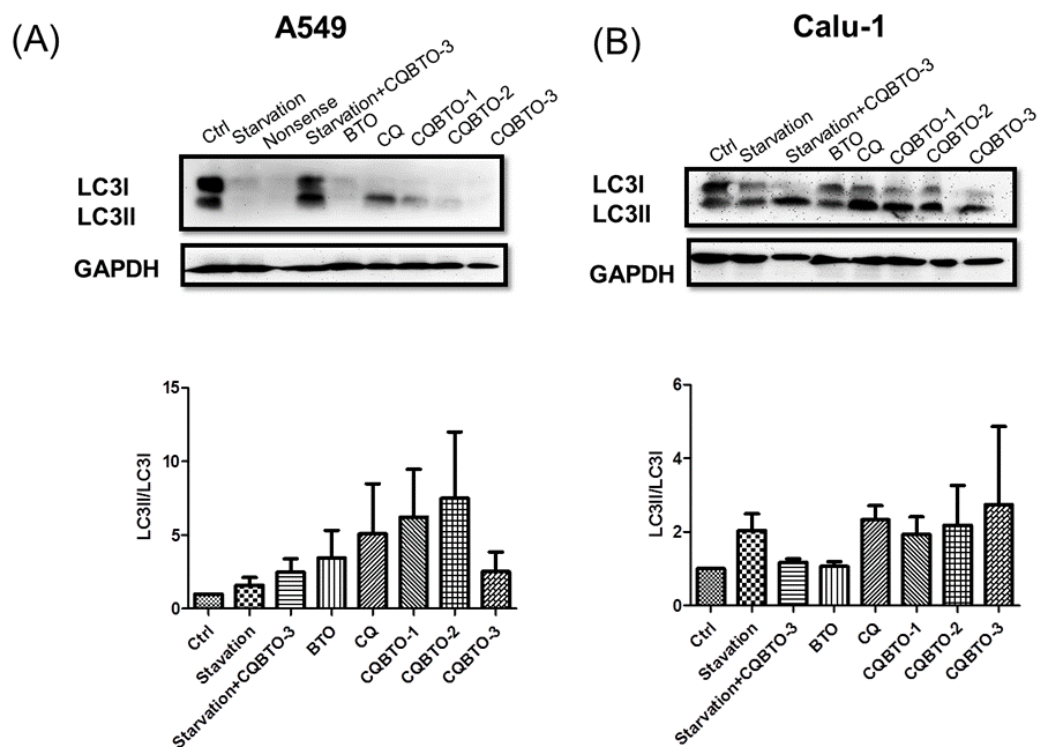


Figure 4

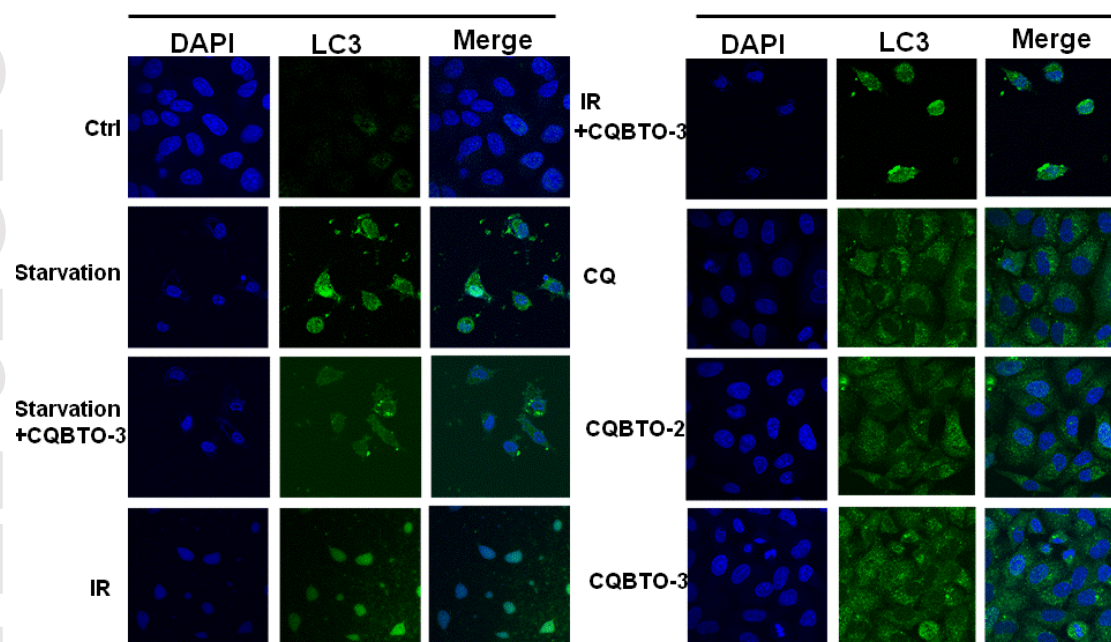
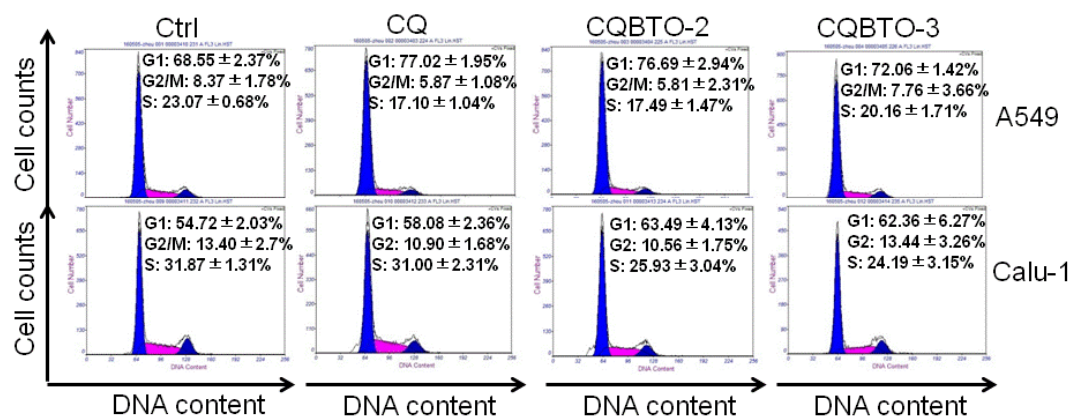


Figure 5:

(A)



(B)

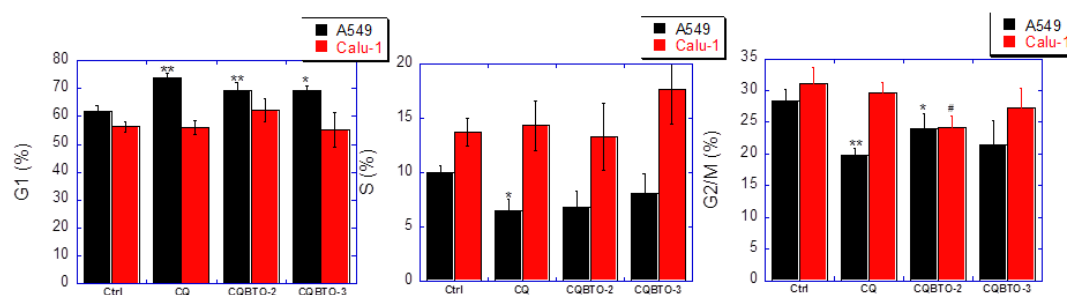


Figure 6

(A)

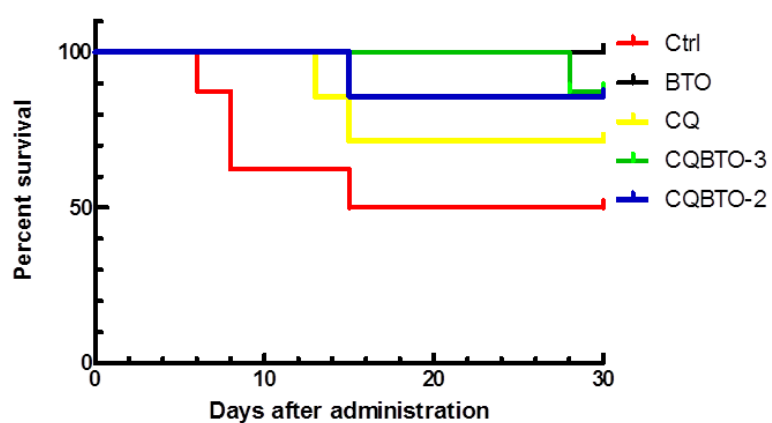


Figure: 6

(B)

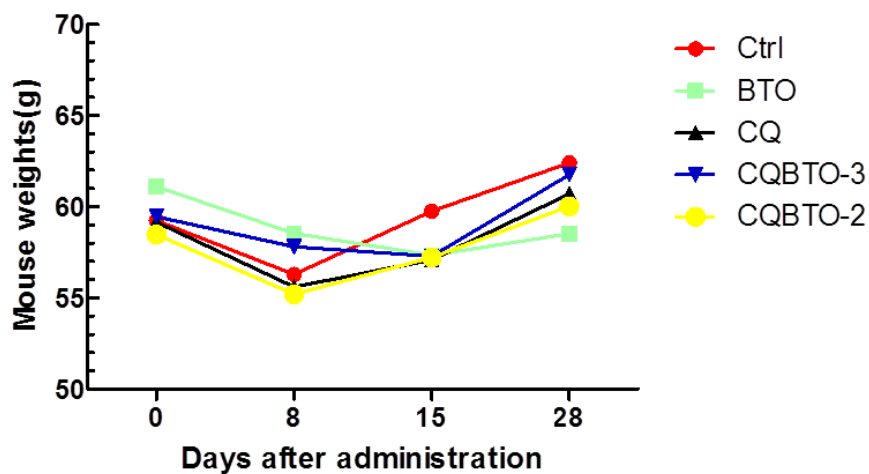


Figure: 6

(C)

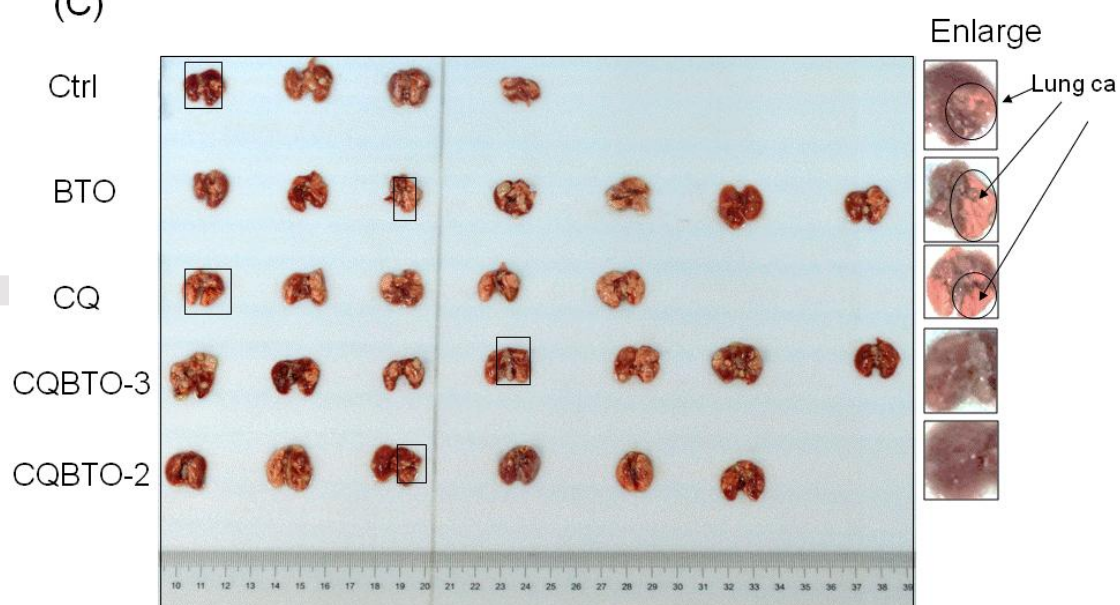


Figure: 6

(D)

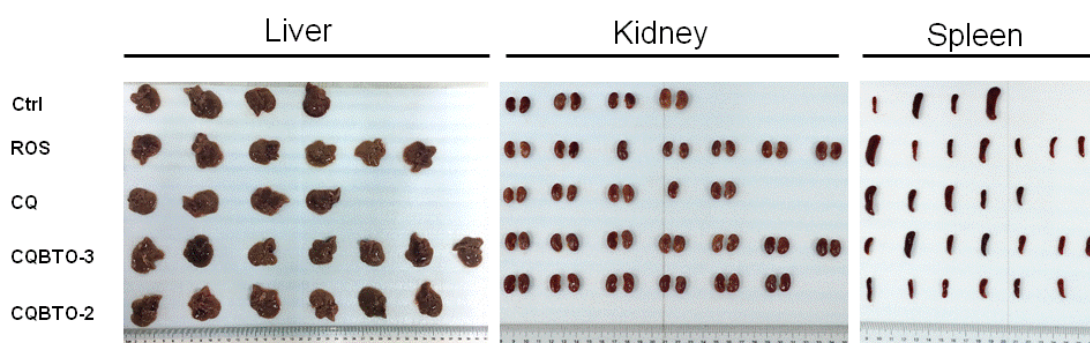


Figure: 6

(E)

